Roller Arrangement Problem of Omnidirectional Mobil Robot Adapted Three Omni Rollers

Kenji Kimura
Department of Control Engineering, National Institute of Technology, Matsue College
14-4 Nishi-ikuma-cho, Matsue-shi,Shimane, 690-8518, Japan

Yuki Shigyo
Digital Solution Div, DX Engagement Dept, Fujitsu
3-5-20 Minamikamata. Ota City, Tokyo, 144-0035, Japan

Kazuo Ishii
Graduate School of Life Science and engineering, Kyusyu Institute of Technology
2-4 Hibikino,Wakamatsu-ku, Kitakyushu 808-0196, Fukuoka, Japan
E-mail:k-kimura@matsue-ct.jp, shigyo.yuki@fujitsu.com , ishii@brain.kyutech.ac.jp

Abstract

Mobile robots adapted to omni rollers are required to have efficient mobility in areas like logistics. Since such systems are easily controlled and provide omnidirectional locomotion. However, theoretical research regarding the motion efficiency has not been conducted. In this study, to evaluate roller arrangements with respect to speed efficiency, a mechanism where the roller placement position can be changed arbitrarily on a round shape mechanism and evaluate the robot speed efficiency is designed. We consider existence domain of the robot speed vector using the theory of linear transformation.

Keywords: Omni-roller, transformation matrix, robot mobile speed

1. Introduction

Recently, efficient mobility has become a requirement for mobile robots in areas like logistics. Thus, omnidirectional movement with either non-holonomic or holonomic characteristics can produce a total of 3 degrees of freedom motion (sum of 2 degrees of freedom translational motion and 1 degree of freedom rotational motion). Robotic vehicle development is getting attention.

Among them, the holonomic movement mechanism is simple to control because of the independently driven wheels and offers outstanding omnidirectional mobility. Thus, A mobile robot arranged in an equilateral triangle has been developed[1].

RV-infinity [2], Musashi150 [3], and NuBot [4] have adopted a mechanism placed in RoboCup MSL, that has three omni rollers arranged in an equilateral triangle. **Figure 1** shows three roller arrangement patterns, and **Figure 1**(i) shows the adopted A-type. Additionally, the types shown in **Figures 1** (ii) and (iii) are also conceivable, but intuitively, they use the most symmetrical triangle arrangement, and theoretical research is unconducted.

In this study, we generalize of equilateral triangle arrangement by assuming a mechanism in which the roller placement position on a round shapes mechanism can be changed arbitrarily. We derive kinematics that generalizes the kinematics in [1] and derives a transformation matrix, which associates input and output. Additionally, we evaluate roller arrangement, focusing on speed efficiency. As approaches, employing the area of robot velocity vector

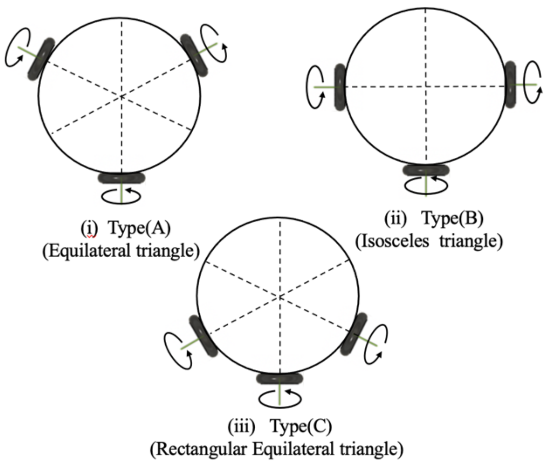

Figure 1 Omni rollers arrangement type of mobile robots in three rollers

as evaluation functions. Kinematics is derived and the linear transformation matrix, associating the input (roller speed) with the output (component of robot movement speed) is employed to measure the image size.

2. Kinematics of mobile robot adapted three omni rollers

This section introduces kinematics, which the roller placement position can be changed arbitrarily.

Assuming horizontal plane movement, the kinematics of both robots is similar. The primary focus lies in the connection between driving omni-wheels rotational speed and robot velocity.

2.1 *Inverse kinematics*

Figure 2 shows a top view of the mobile robot that has a common radius of all omni-wheels adapted The *i-th* rollers ($i = 1,2,3$) contact point $\boldsymbol{P_i}$ on a circle, which has radius R. X-Y is the global coordinate system (origin $\boldsymbol{O}$) and $\acute{X}$-$\acute{Y}$ is robot coordinate system(origin $\acute{\boldsymbol{O}}$). And. The robot orientation ϕ is referred as the angle between X-axis and $\acute{X}$-axis. and the distance from the robot center to the contact points between wheels and floor is R.

$\{\boldsymbol{e_1}, \boldsymbol{e_2}, \boldsymbol{e_3}\}$ represents the normal vector of rotational direction.

We compute the roller peripheral speed v_i that gives the robot translation speed $\boldsymbol{V} = [V_x, V_y]^{\boldsymbol{T}}$ and φ denotes the robot direction for the robot coordinate $\acute{X}$-$\acute{Y}$ and the robot rational speed $L\dot{\phi}$ ($\dot{\phi}$: robot angular velocity) and the roller peripheral speed v_i are decomposed translation and rotational components.

Rollers contact point $\boldsymbol{P_i}$ are the adapted angle θ_i measured from x-axis on the circle and has a radius L.

$$\boldsymbol{P_i} = L[\cos\theta_i, \sin\theta_i]^{\boldsymbol{T}} \tag{1}$$

Rollers velocity vector $\boldsymbol{e_i}$ is perpendicular to $\boldsymbol{P_i}$.

$$\boldsymbol{e_i} = [-\sin\theta_i, \cos\theta_i]^{\boldsymbol{T}} \tag{2}$$

v_i is represented as the sum of the translation component $\langle \boldsymbol{e_i}, [V_x, V_y]^{\boldsymbol{T}} \rangle$ and rotational component $L\dot{\phi}$.

$$v_i = \langle \boldsymbol{e_i}, [V_x, V_y]^{\boldsymbol{T}} \rangle + L\dot{\phi} \tag{3}$$

Thus, $[v_1, v_2, v_3]^{\boldsymbol{T}}$ is represented as follows.

$$\begin{bmatrix} v_1 \\ v_2 \\ v_3 \end{bmatrix} = \begin{bmatrix} -\sin\theta_1 & \cos\theta_1 & 1 \\ -\sin\theta_2 & \cos\theta_2 & 1 \\ -\sin\theta_3 & \cos\theta_3 & 1 \end{bmatrix} \begin{bmatrix} V_x \\ V_y \\ L\dot{\phi} \end{bmatrix} \tag{4}$$

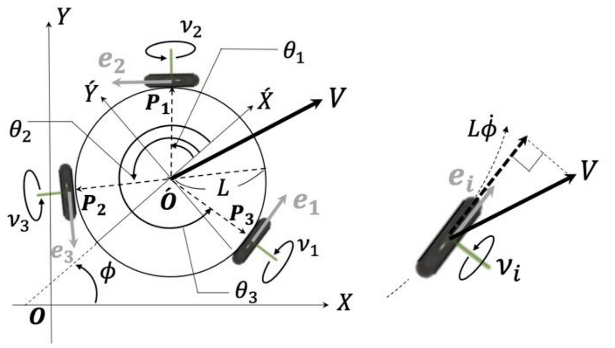

Figure 2 A top view of the mobile robot for kinematics.(i) Parameter list two coordinates (ii).Single rollers motion.

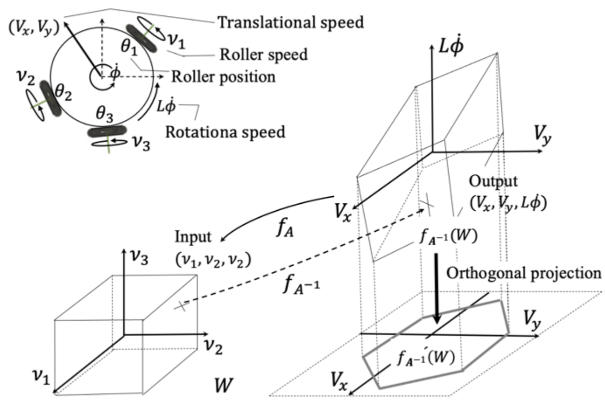

Figure 3 Structural transformation between the three rollers, robot mobile speed (V_x, V_y), and rotational speed $L\dot{\phi}$.

2.2 *Forward kinematics*

Eq.(4) is solved to $[V_x, V_y, L\dot{\phi}]^T$ as following;

$$\begin{bmatrix} V_x \\ V_y \\ L\dot{\phi} \end{bmatrix} = \frac{1}{\det\boldsymbol{A}} \cdot \tag{5}$$

$$\begin{bmatrix} \cos\theta_2 - \cos\theta_3 & -\cos\theta_1 + \cos\theta_3 & \cos\theta_1 - \cos\theta_2 \\ \sin\theta_2 - \sin\theta_3 & -\sin\theta_1 + \sin\theta_3 & \sin\theta_1 + \sin\theta_2 \\ \sin(\theta_3 - \theta_2) & \sin(\theta_1 - \theta_3) & \sin(\theta_2 - \theta_1) \end{bmatrix} \begin{bmatrix} v_1 \\ v_2 \\ v_3 \end{bmatrix}$$

Where

$$\det\boldsymbol{A} = \sin(\theta_3 - \theta_2) + \sin(\theta_1 - \theta_3) + \sin(\theta_2 - \theta_1) \tag{6}$$

3. Evaluation function focus on robot speed vector area

In this section, the roller contact location is calculated using the orthogonal projection area of image as evaluation functions.

Figure 3 shows a cubic domain that has a square, 2 $[m/s]$ on each side and the volume, 8 $[m/s]^3$ as input.

$$W = \{(v_1, v_2, v_3) \mid |v_1|, |v_2|, |v_3| \le 1\} \tag{7}$$

Here, from linear transformation mapping $f_{A^{-1}} : [v_1, v_2, v_3] \to [V_x, V_y, \dot{\phi}L]$, $f_{A^{-1}}(W) \in \mathbf{R}^3$ is a parallelepiped domain as follows (linear transformation matrix $\boldsymbol{A}$, $\det \boldsymbol{A}^{-1}$ is equal to $1/\det \boldsymbol{A}$. It is the volume ratio). Using $\boldsymbol{A}^{-1} = [\boldsymbol{A_1}, \boldsymbol{A_2}, \boldsymbol{A_2}]$, $f_{A^{-1}}(W)$ is represented as follows.

$$f_{A^{-1}}(W) = \tag{8}$$

$$\{(V_x, V_y, L\dot{\phi}) \mid v_1\boldsymbol{A_1} + v_2\boldsymbol{A_2} + v_3\boldsymbol{A_3},\ |v_1|, |v_2|, |v_3| \le 1\}$$

Next, Using the projection vector of $\boldsymbol{A_i}$ with respect to V_x, V_y-plane, we define the orthographic projection domain $\acute{f}_{A^{-1}}(W)$ for horizontal plane as follows.

$$\acute{f}_{A^{-1}}(W) = \tag{9}$$

$$\{(V_x, V_y) \mid v_1\acute{\boldsymbol{A}}_1 + v_2\acute{\boldsymbol{A}}_2 + v_3\acute{\boldsymbol{A}}_3,\ |v_1|, |v_2|, |v_3| \le 1\}$$

Thus the orthographic projection area $D_{Are}(\theta_1, \theta_2, \theta_3)[m/s]^2$ is represented as sum of parallelogram area $I(\ ,\ )$;

$$D_{Are} = \begin{cases} 4I(\acute{\boldsymbol{A}}_1, \acute{\boldsymbol{A}}_2) + 4I(\acute{\boldsymbol{A}}_1 - \acute{\boldsymbol{A}}_2, \acute{\boldsymbol{A}}_3) \\ \qquad [\,(\acute{\boldsymbol{A}}_2 \times \acute{\boldsymbol{A}}_3)_z (\acute{\boldsymbol{A}}_1 \times \acute{\boldsymbol{A}}_3)_z < 0] \\ 4I(\acute{\boldsymbol{A}}_1, \acute{\boldsymbol{A}}_2) + 4I(\acute{\boldsymbol{A}}_1 + \acute{\boldsymbol{A}}_2, \acute{\boldsymbol{A}}_3) \\ \qquad [\,(\acute{\boldsymbol{A}}_2 \times \acute{\boldsymbol{A}}_3)_z (\acute{\boldsymbol{A}}_1 \times \acute{\boldsymbol{A}}_3)_z > 0] \end{cases} \tag{10}$$

where

$$\acute{\boldsymbol{A}}_1 = \begin{bmatrix} \cos\theta_2 - \cos\theta_3 \\ \sin\theta_2 - \sin\theta_3 \\ 0 \end{bmatrix},\ \acute{\boldsymbol{A}}_2 = \begin{bmatrix} -\cos\theta_1 + \cos\theta_3 \\ -\sin\theta_1 + \sin\theta_3 \\ 0 \end{bmatrix}$$

$$\acute{\boldsymbol{A}}_3 = \begin{bmatrix} \cos\theta_1 - \cos\theta_2 \\ \sin\theta_1 + \sin\theta_2 \\ 0 \end{bmatrix} \tag{11}$$

Theoretically, we find out that D_{Are} was minimized in the equilateral triangle arrangement (Case of type(A)).

4. Simulation

This section presents the simulation findings, including the evaluation values of behavior and shape of orthogonal projection area D_{Are} and we assume that $L = 1[\mathrm{m}]$.

4.1 *Behavior of the evaluation function*

Figure 4 shows evaluation function D_{Are} when the symmetry arrangement is with respect to y-axis (substituting Eq.(10) with $\theta_1 = \theta$, $\theta_2 = 180° - \theta$, and $\theta_3 = 270°$, $-90° \le \theta \le 90°$).

D_{Are} takes the minimal value when $\theta = 30°$ (case of equilateral triangle arrangement).

4.2 *Shape of orthographic projection area*

Simulations were performed at the three various roller arrangement patterns that $\boldsymbol{P_1}$, $\boldsymbol{P_2}$ and $\boldsymbol{P_3}$ are arranged a symmetry triangle shaped(See Figure1).

They are set up θ_i $(i = 1,2,3)$ as follows:

Type(A): $(\theta_1, \theta_2, \theta_3) = (30°, 150°, 270°)$

Type(B): $(\theta_1, \theta_2, \theta_3) = (0°, 180°, 270°)$

Type(C): $(\theta_1, \theta_2, \theta_3) = (210°, 270°, 300°)$

Figure 5 shows an outlines of robot velocity distributions for Type(A), Type(B), and Type(C).

It shows that the orthogonal projections on the parallelepiped's horizontal planes are all hexagons.

Table 1 shows the area D_{Are} on the horizontal plane $V_x - V_y$ of the parallelepiped as evaluation values.

Type (A) is the smallest. Additionally, since Type(C) is the largest, the moving area for the translational motion

Table 1 Comparison of the evaluation value

	Type (A)	Type (B)	Type (C)
D_{Are} $[m/s]^2$	4.61	6.00	13.85

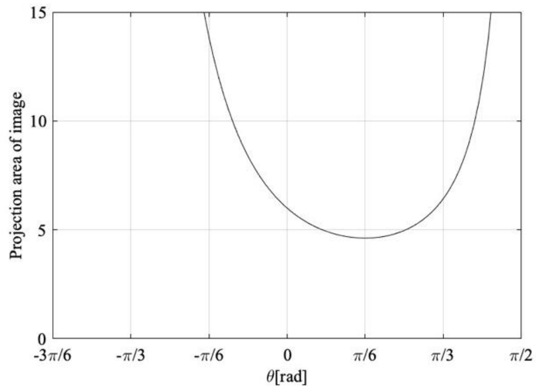

Figure 4 Behavior of evaluation function D_{Are} $[m/s]^2$

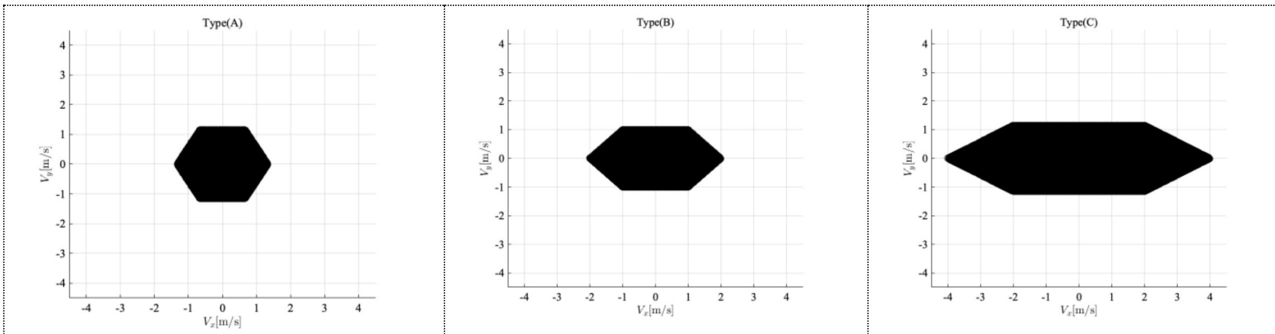

(i) Case of Type (A) (ii) Case of Type (B) (iii) Case of Type (C)

Figure 5 Projection domain of $f_{A^{-1}}(W)$ on horizontal plane (V_x, V_y)

is effective. Therefore, results were obtained for the evaluation.

5. Conclusions

In this research, we derived the kinematics of a mechanism that can arbitrarily change the roller placement position on a circle and considered the roller placement using the transformation matrix, associating input and output as an evaluation function.

As a result, theoretically, for Case of type(A), we find out that evaluation function was minimized in the equilateral triangle arrangement. Furthermore, in terms of translational motion, type(C) is the most efficient comprehensively among the three types.

References

[1] J.Tang, K.Watanabe, et al., "Autonomous control for an omnidirectional mobile robot with the orthogonal-wheel assembly," Journal of the Robotics Society of Japan. Vol. 17, No. 1,pp. 51-60, 1999.

[2] Y.Yasohara, K.Shimizu, et al., "Development of ball handling mechanism for RoboCup MSL," *30th Fussy System Symposium*, pp. 616-617, 2014.

[3] S.Chikushi, M.Kuwada, et al., "Development of next-generation soccer robot "Musashi150"for RoboCup MSL, *30th Fussy System Symposium*, pp. 624-627, 2014

[4] R.Junkai, X.Chenggang, X.Junhao, et al., "A control system for active ball handling in the RoboCup middle size League,"*Chinese Control and Decision Conference(CCDC.)2016.*

Authors Introduction

Dr. Kenji Kimura

He is a lecturer in the Department of Control Engineering, National Institute of Technology, Matsue College starting in 2022. He received the ME (mathematics) from Kyushu University in 2002 and received his Ph.D. degree in engineering from Kyushu Institute of in 2020. His research interests include spherical robot, control for object manipulation, and Riemannian geometry.

Mr. Yuki Shigyo

He is an engineer working for Fujitsu Ltd. He received the BE from Tokyo University of Science in 2016 and the ME (mathematics) from Nagoya University in 2018. His research interests are spherical mobile robot kinematics and machine learning.

Dr. Kazuo Ishii

He has been a professor at the Kyushu Institute of Technology since 1996. He received his Ph.D. degree in engineering from the University of Tokyo, Tokyo, Japan, in 1996. His research focuses on ship marine engineering and intelligent mechanics. He holds five patents derived from his research.